Structure

Article

Off-target reactivity in clinical monoclonal antibodies

Graphical abstract

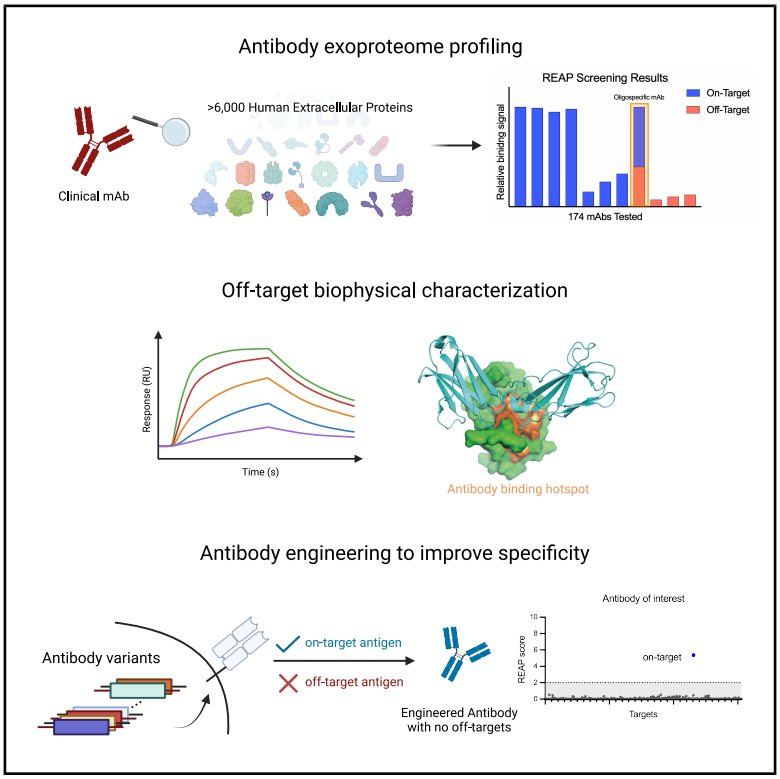

Highlights

- An unprecedented systematic assessment of off-target reactivity in clinical antibodies
- Identifying functional off-targets that disrupt receptor-ligand signaling
- Development of a generalizable engineering approach to eliminate off-target binding

Authors

Yile Dai, Joseph Brouillard, Jillian R. Jaycox, ..., Arvind Sivasubramanian, James C. Geoghegan, Aaron M. Ring

Correspondence

arvind.sivasubramanian@adimab.com (A.S.), jcgeoghegan@gmail.com (J.C.G.), aaronring@fredhutch.org (A.M.R.)

In brief

Dai et al. present a large-scale analysis of off-target binding in clinical-stage therapeutic antibodies. Their findings reveal an unexpectedly high prevalence of specific off-target interactions and show how antibody engineering can reduce these risks, emphasizing the value of early specificity screening in biologic drug development.

Dai et al., 2026, Structure *34*, 1–11
May 7, 2026
https://doi.org/10.1016/j.str.2026.02.012

CellPress

Please cite this article in press as: Dai et al., Off-target reactivity in clinical monoclonal antibodies, Structure (2026), https://doi.org/10.1016/j.str.2026.02.012

Structure

CellPress

Article

Off-target reactivity in clinical monoclonal antibodies

Yile Dai,[1,8] Joseph Brouillard,[4,8] Jillian R. Jaycox,[1,3] Sung M. Yeon,[1,3] John D. Huck,[1] Soumya S. Yandamuri,[1,2] Zhe Zhong,[1] Kevin C. O'Connor,[1,2] Irina Burnina,[5] Cameron Henkel,[6] Allie K. LeMay,[5] Asparouh Lilov,[5] Elizabeth McGurk,[5] Morgan Morrill,[7] Liz Parker,[5] Tricia Sackett,[7] Chanita Sandberg,[7] Arvind Sivasubramanian,[4,6,*] James C. Geoghegan,[4,*] and Aaron M. Ring[3,9,*]

[1]Department of Immunobiology, Yale School of Medicine, New Haven, CT 06511, USA
[2]Department of Neurology, Yale School of Medicine, New Haven, CT 06511, USA
[3]Translational Science and Therapeutics Division, Fred Hutchinson Cancer Center, Seattle, WA 98109, USA
[4]Platform Technologies, Adimab LLC, Lebanon, NH 03766, USA
[5]Protein Analytics, Adimab LLC, Lebanon, NH 03766, USA
[6]Computational Biology, Adimab LLC, Lebanon, NH 03766, USA
[7]High Throughput Expression, Adimab LLC, Lebanon, NH 03766, USA
[8]These authors contributed equally
[9]Lead contact
*Correspondence: arvind.sivasubramanian@adimab.com (A.S.), jcgeoghegan@gmail.com (J.C.G.), aaronring@fredhutch.org (A.M.R.)
https://doi.org/10.1016/j.str.2026.02.012

SUMMARY

Biologics, including monoclonal antibodies (mAbs), are widely used therapeutics due to their high specificity, yet off-target interactions remain an underappreciated risk for safety and efficacy. To systematically assess antibody specificity, we applied rapid extracellular antigen profiling (REAP) to evaluate 174 FDA-approved and clinical-stage antibodies against 6,172 human extracellular proteins. We found a substantial burden of off-target reactivity, with 28% of antibodies exhibiting at least one off-target hit. Structural and biophysical analyses revealed that off-target binding arises from antibody intrinsic properties and epitope mimicry, either within related protein families or across structurally unrelated proteins. We further identified new off-target interactions of tanezumab and engineered its variable domains to eliminate off-target binding while preserving target affinity and developability. These findings highlight the prevalence of specific off-target reactivity in therapeutic antibodies and underscore the importance of evaluating specificity early in biologic drug development.

INTRODUCTION

Antibody therapeutics represents the largest class of biologic drugs, with over 130 approved molecules over the last two decades.[1] Despite their advantages in target specificity, stability, solubility, and ease of manufacturing compared to other therapeutic classes, antibodies frequently fail during development due to factors not directly related to their intended disease-modifying effects. Beyond traditional metrics of antibody "developability," there is growing recognition that antibodies may have more off-target reactivity than previously appreciated. These off-target reactivities pose significant clinical risk not just for conventional antibody therapeutics, but for emerging antibody-containing modalities with augmented potency such as T cell engagers and chimeric antigen receptor (CAR) T cells where even low-affinity binding can result in powerful biological activity.

One mode of off-target binding occurs with antibodies that exhibit non-specific binding to multiple antigens, often referred to as polyreactive or "sticky" antibodies. Polyreactive antibodies can be readily identified using assays such as the polyspecificity reagent (PSR) assay, baculovirus particle (BVP) assay, polyreactivity ELISA, and heparin column chromatography.[2,3] These assays vary in throughput but all can be readily implemented during the discovery phase to exclude antibodies with poor biophysical properties. Additionally, non-specific polyreactivity can be driven by predictable features such as electropositive or hydrophobic patches within the variable domains and/or conformational instability within the complementary determining regions (CDRs), leading to promiscuous binding.[4–6]

A more insidious type of off-target binding occurs when antibodies can bind to multiple, unrelated antigens in a specific manner.[7] These antibodies are referred to as oligospecific.[8] *In vivo*, antibodies with reactivity to self-proteins are depleted from the repertoire via central tolerance.[9] However, as most therapeutic antibodies are derived from animal immunization or *in vitro* display libraries, and are frequently engineered for enhanced activity, there is an increased possibility of isolating antibodies with specific off-target reactivities, including to human proteins. There have been several reports of oligospecific

Please cite this article in press as: Dai et al., Off-target reactivity in clinical monoclonal antibodies, Structure (2026), https://doi.org/10.1016/j.str.2026.02.012

antibodies, including cases where off-target binding conferred toxicity or negatively impacted pharmacokinetics.[10–12] Screening for specific off-target binding is more challenging than detecting non-specific polyreactivity as it requires a system that can probe binding interactions between an antibody and the thousands of unique extracellular proteins or protein domains that may be encountered *in vivo*. Furthermore, the molecular determinants of oligospecificity are not well understood and are unlikely to be readily generalizable like polyreactivity. Importantly, the overall prevalence of oligoreactivity is understudied, with limited reports on sets of antibodies and largely unknown beyond anecdotal reports for individual antibodies.[10,13,14]

Here, we leveraged the REAP platform—a yeast display-based screening system that enables conformational epitope interaction analysis with >6,000 human extracellular proteins and protein domains[15]—to profile the specificity of 174 clinical-stage monoclonal antibodies. We found that while most tested antibodies show no detectable off-targets, more than one-quarter exhibited interaction with at least one non-target protein, with most examples being oligospecific. We describe the off-target interaction for NGF antibody tanezumab, which showed unexpected binding to the thymic stromal lymphopoietin (TSLP). Through epitope mapping and biochemical competition assays, we found that tanezumab binds to an epitope that overlaps with the natural binding interface between TSLP and its receptor, TSLPR (CRLF2)[16] and competes for binding with the approved anti-TSLP blocking antibody, tezepelumab.[17] We additionally demonstrate that CDR engineering can readily remove off-target reactivities while maintaining or improving affinity toward the intended target, consistent with prior reports.[18]

This study presents a new platform enabling high-throughput specificity screening of monoclonal antibodies coupled with a generalizable engineering approach to ablate off-target binding (graphical abstract). In addition, our results highlight the value of discovery-stage screening to inform rank ordering of clinical candidates and the potential need for specificity engineering to mitigate developability risks. Finally, REAP screening can reveal unexpected interactions which could confer biological activities either related to or distinct from the antibodies' therapeutic mechanism of action.

RESULTS

REAP screen of clinical-stage antibodies

Using REAP, we profiled a total of 174 FDA-approved or clinical-stage mAbs against 6,172 human extracellular proteins composed of full-length conformational antigens and linear epitopes (Figure 1A). All antibodies included in the study are monospecific IgGs, with two exceptions; emicizumab is a bispecific antibody and brentuximab vedotin is an antibody-drug conjugate. Initially, we screened 29 EU-licensed, therapeutic mAb drug aliquots sourced from Evidentic GmbH. All target antigens corresponding to these antibodies were represented in the REAP library with the exception of the respiratory syncytial virus fusion protein, which is targeted by palivizumab. REAP analysis detected binding to their intended antigens for 21 of the 28 mAbs (75.0%; palivizumab excluded), validating the technique's fidelity and performance in presenting the majority of extracellular antigens in their correct conformation. Of the seven antibodies that did not show interaction with their cognate antigen, three bind the multipass membrane protein CD20, one binds factor X and activated factor IX, and the remaining three bind α4β7 integrin heterodimer, EGFR, and ERBB2, respectively. In addition to on-target reactivities, we detected off-target reactivities for five mAbs (Figures 1B and 1C, Data S3). Of these off-target reactivities, we selected the binding of pembrolizumab (anti-PD-1) to teratocarcinoma-derived growth factor 1 (TDGF1) for further validation (Figure 1B). Binding to TDGF1 was confirmed by an enzyme-linked immunosorbent assay (Figure S1).

Next, we screened an additional 80 FDA-approved and 65 clinical-stage mAbs. Of these 145, 15 were commercially sourced biosimilars. The remaining 130 were formatted and expressed as IgG1 isotype mAbs regardless of the original drug isotype, with variable domains matching published sequences. The HC isotype of the clinical mAb is IgG1 in 78 out of 130 cases, with 16 cases being IgG2, 33 IgG4, and three mixed isotype. For simplicity, we generally use the INNs (e.g., tanezumab) to refer to the samples, with the understanding that our sample is not identical to the original clinical material. We selected the 145 mAbs based on their full-length IgG format and a diversity of clinical stages and targets. We also included examples of distinct mAbs that recognize the same target to determine if there were antigen-dependent patterns in the off-target interactions. Of the total 174 mAbs analyzed, 126 (72%) showed no off-target reactivity, aligning with the expected high specificity of mAbs advanced to clinical testing. However, 30 of the 174 mAbs (17%) showed off-target reactivity toward one antigen, and 18 mAbs (10%) bound to at least two off-targets, representing oligospecific binding patterns (Figures 1D and 1E, Data S3, and S4). Notably, aducanumab, lecanemab, solanezumab, anselamimab, and gantenerumab, all targeting amyloid-beta (Aβ) peptides, exhibited apparent polyreactivity, binding a large number of off-target antigens (5, 6, 8, 11, and 44, respectively), potentially reflecting the inherent promiscuous biochemical behavior associated with mAbs recognizing amphipathic Aβ peptides.

To understand the relationship between REAP-identified interactions and biophysical properties potentially associated with off-target binding, we analyzed all IgG samples by hydrophobic interaction chromatography (HIC) and PSR assays.[19] We did not observe a correlation between HIC retention time and the number of off-target reactivities as measured by REAP (Data S5). The median PSR score of antibodies with two or more REAP-identified off-targets is higher than that for antibodies with no identified off-targets (0.42 vs. 0.11) (Figure 1F). 74% of antibodies (14/19) with a PSR score above 0.33, a threshold previously reported for high PSR reactivity,[20] return one or more off-target hits compared to 22% (34/155) for antibodies with PSR values below this threshold. Antibodies targeting Aβ represent half of the subset with elevated PSR and at least one identified off-target. The Aβ antibodies gantenerumab and anselamimab have relatively high PSR scores (0.53 and 0.38, respectively) in contrast to solanezumab, which showed no polyreactivity in the PSR assay (Data S5). While the PSR score does not directly correlate to the number of off-targets identified by REAP, it has a modest predictive value (area under ROC value of 0.69; data not shown) in identifying antibodies with at least one off-target.

Please cite this article in press as: Dai et al., Off-target reactivity in clinical monoclonal antibodies, Structure (2026), https://doi.org/10.1016/j.str.2026.02.012

CellPress

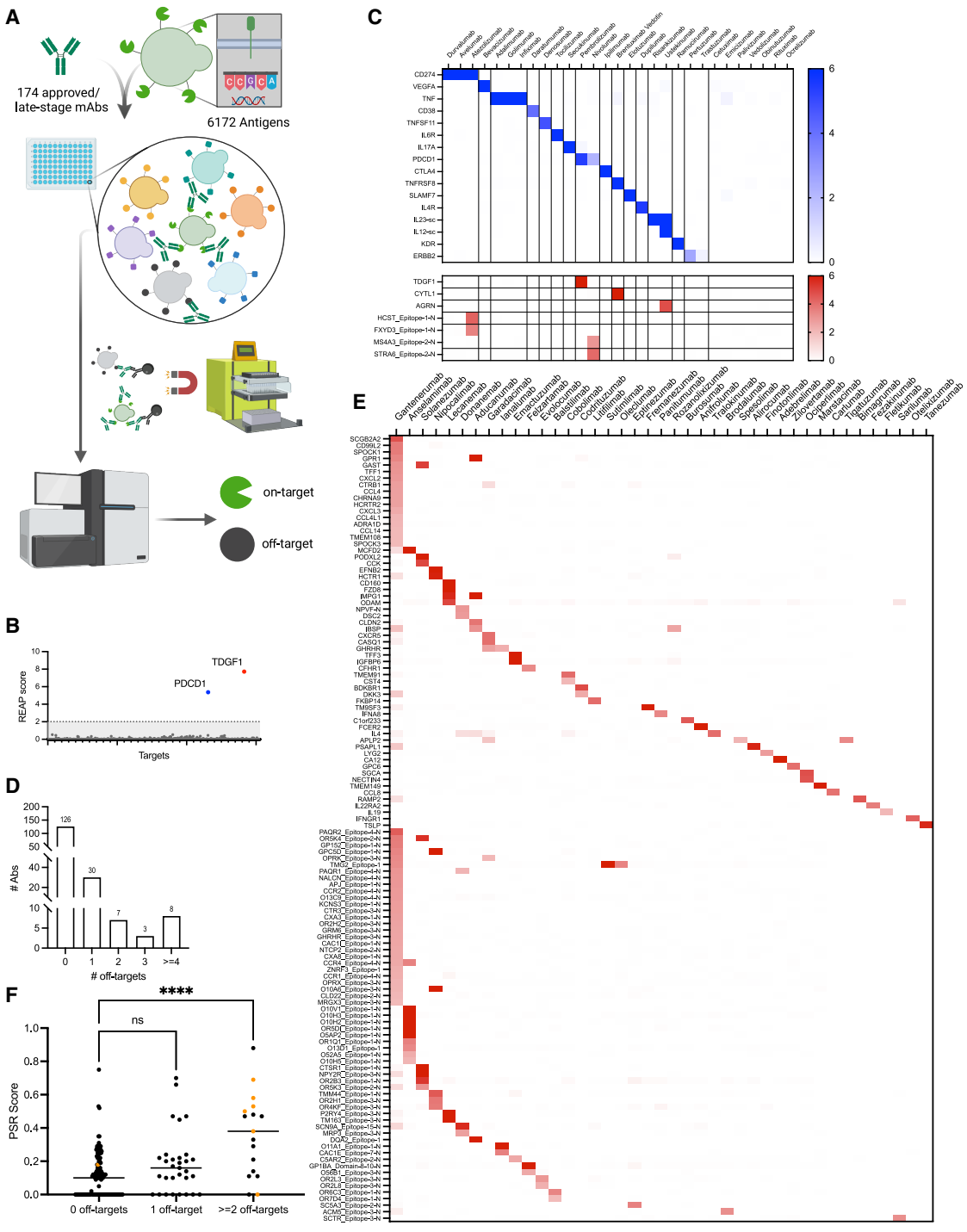

Figure 1. REAP screen of clinical-stage antibodies

(A) Schematic of REAP workflow of 174 antibodies screened against a library of 6,172 antigens.

(B) Pembrolizumab shows binding to its target PDCD1 (blue) and one off-target, TDGF1 (red).

(C) 29 clinical-grade antibody samples were screened in REAP, and 21 bound their intended antigens (13 cell-surface, seven secreted, and one viral), shown in blue. Off-target interactions identified by REAP are shown in the lower section in red.

(D) Of all 174 antibodies tested, 72% did not show any off-target reactivities, 17% show one reactivity, and 10% show two or more.

(E) REAP screening results of an additional 41 antibodies out of 145 non-clinical grade antibody samples with at least one off-target.

(legend continued on next page)

Please cite this article in press as: Dai et al., Off-target reactivity in clinical monoclonal antibodies, Structure (2026), https://doi.org/10.1016/j.str.2026.02.012

Table 1. BLI validation of REAP-predicted off-target interactions

IgG	Protein	Uniprot ID	Type	REAP score	K_D (M) avid	Binding response (nm)
Tanezumab	TSLP	Q969D9	Secreted	5.70	6.90E-08	0.16
Otelixizumab	IFNGR1	P15260	SP type I	4.34	Poor fit	0.42
Emactuzumab	TFF3	Q07654	Secreted	8.58	Poor fit	0.74
Adebrelimab	CA12	O43570	SP type I	7.67	Poor fit	0.41
Pembrolizumab	TDGF1	P13385	GPI anchored	7.72	Poor fit	0.36
Lecanemab	CD160	O95971	GPI anchored	7.03	8.72E-07	0.23
Tralokinumab	IL4	P05112	Secreted	4.06	2.93E-09	0.48
Ociperlimab	NECTIN4	Q96NY8	SP type I	4.67	3.16E-09	0.44
Panitumumab	IFNA8	P32881	Secreted	3.41	Poor fit	0.12

Summary of avid binding measurements and binding responses derived from biolayer interferometry assay for a subset of antibody-antigen interactions identified by REAP. Apparent K_D values are not reported for interactions where either no or weak binding (<0.1 nm response) was observed, or the binding could not be fit to a 1:1 binding model (Poor fit). Related to Figures 2 and 3.

Biochemical validation of off-target reactivities identified by REAP

To validate the results from the REAP screen, we selected a subset of identified interactions to assess by an orthogonal binding assay. Recombinant soluble forms of nine proteins that interacted with nine IgGs were tested for binding by Octet biolayer interferometry (BLI) assay (Table 1). These included secreted, single-pass type I, and GPI-anchored proteins. All nine of the proteins exhibited binding to the associated IgG (Table 1 and Figure S2). In four cases an apparent affinity could be derived, while in five cases the observed binding was detectable but either too weak or could not be fit to a 1:1 binding model to obtain an equilibrium dissociation constant (Table 1 and Figure S2).

Tralokinumab, an anti-interleukin 13 (IL13) antibody, demonstrated binding to interleukin 4 (IL4) (Figures 2A and 2B). IL13 and IL4 share only 28% overall sequence identity, but are structurally related members of the short-chain interleukin class.[21] The off-target reactivity is potentially explained by the fact that IL13 and IL4 share some identical or conserved amino acids in the defined tralokinumab epitope positions.[22] Ociperlimab, an anti-TIGIT antibody, exhibited binding to nectin-4 (NECTIN4) (Figure 2C). TIGIT and NECTIN4 are structurally related proteins containing an Ig-like V-type domain with approximately 26% sequence identity. However, 40% of the reported ociperlimab epitope amino acids on TIGIT,[23] including a histidine at position 76 that confers pH-dependent binding,[23] are identically present in the NECTIN4 3D structure (Figure 2D).[24] This structural mimicry could potentially explain the observed cross-reactivity of ociperlimab. Given that ociperlimab is known to display enhanced binding to TIGIT at low pH,[23] we investigated whether ociperlimab also exhibits pH-dependent binding to NECTIN4 by assessing its binding at pH 7.4 and pH 6.0. Interestingly, stronger binding to NECTIN4 was observed at pH 6.0, suggesting that histidine 89 in NECTIN4, which aligns with histidine 76 in TIGIT, mediates the pH-dependent binding to this off-target protein (Figure 2E).

In summary, all nine of the tested interactions identified by REAP were confirmed by BLI binding assay using soluble recombinant forms of the off-target proteins.

Functional impacts of off-target binding on receptor-ligand interactions

Next, we conducted additional characterization of off-target interactions identified for two oligospecific mAbs, tanezumab and otelixizumab. Tanezumab is a humanized clinical-stage anti-NGF antibody that has been evaluated for treatment of osteoarthritis and pain.[25] TSLP was detected as a top binding hit in the REAP screen of tanezumab (REAP score = 5.7). BLI analysis revealed an apparent affinity ($K_{D,APP}$) of 69 nM when tested in an avid binding format in which TSLP was immobilized on the sensor and tanezumab IgG was applied in solution (Table 1 and Figure S2). Monovalent binding was not observed, indicating the intrinsic affinity of tanezumab for TSLP is weak (Figure S3A). To test whether tanezumab could block the interaction between TSLP and TSLPR, we performed a BLI competition assay (Figures 3A–3D). First, we confirmed that both TSLPR and tezepelumab (an anti-TSLP antibody approved for the treatment of asthma)[26] bind to TSLP with high affinity (Figures S3B and S3C) and that tezepelumab could be detected to block binding of TSLPR to TSLP in this assay system (Figure 3A). Tanezumab also blocked TSLPR binding to TSLP, whereas a negative control antibody did not (Figures 3B and 3C). Pre-complexing TSLP with tezepelumab blocked subsequent binding of tanezumab, indicating that the antibodies share overlapping or proximal epitopes (Figure 3D). These results are consistent with previous reports that off-target binding can modulate natural receptor-ligand interactions, as was found for the anti-PD-1 antibody camrelizumab and its off-target inhibition of VEGFA:VEGFR2.[10]

Not every off-target binding interaction may involve putatively relevant epitopes. Otelixizumab is a humanized anti-CD3ε antibody developed for treatment of autoimmune disorders including type 1 diabetes.[27] To expand our analysis of antibodies that may interfere with off-target ligand-receptor interactions, we

(F) The PSR score of each sample is plotted against the number of off-targets by bin (0 off-targets, 1 off-target, and ≥2 off-targets). Antibodies with two or more identified off-targets showed elevated PSR values relative to antibodies with no identified off-targets. Statistical comparisons made by two-sided Kruskal-Wallis tests with Dunn's correction for multiple comparisons. ****, $p < 0.0001$; n.s., not significant. The orange data points represent the antibodies targeting amyloid-beta related proteins.

Please cite this article in press as: Dai et al., Off-target reactivity in clinical monoclonal antibodies, Structure (2026), https://doi.org/10.1016/j.str.2026.02.012

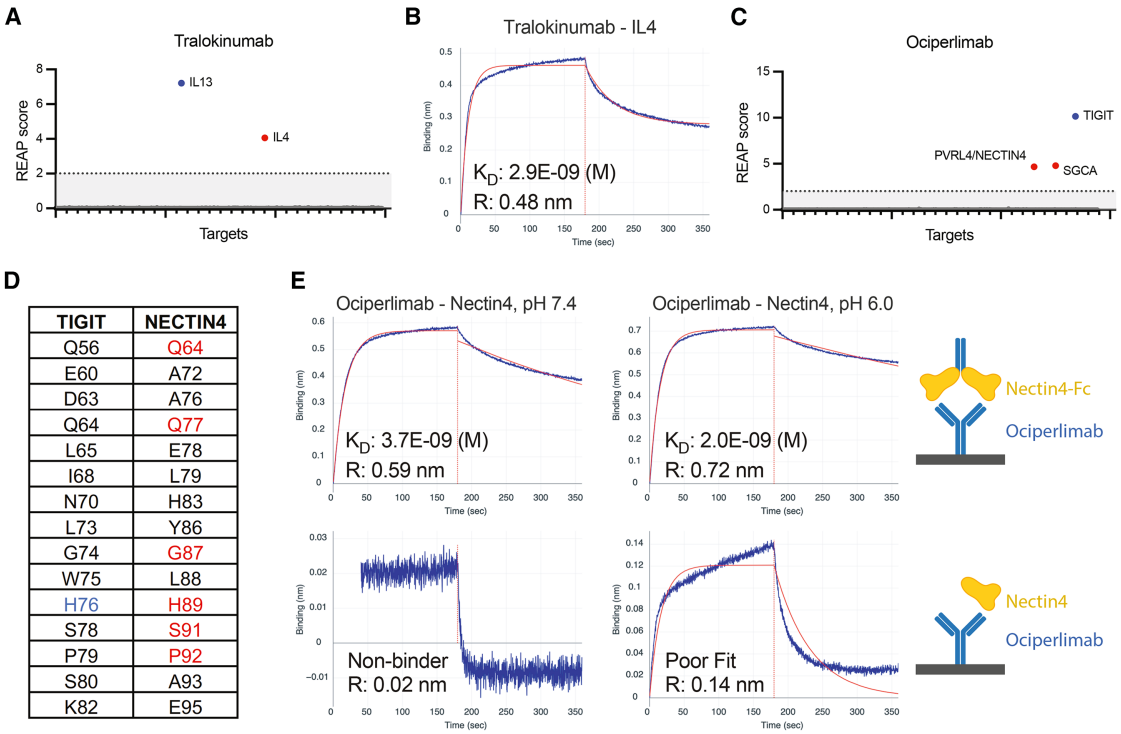

TIGIT	NECTIN4
Q56	Q64
E60	A72
D63	A76
Q64	Q77
L65	E78
I68	L79
N70	H83
L73	Y86
G74	G87
W75	L88
H76	H89
S78	S91
P79	P92
S80	A93
K82	E95

Figure 2. Binding characterization of a subset of antibody-antigen interactions identified by REAP

(A) Tralokinumab shows binding to its target IL13 (blue) and one off-target, IL4 (red).

(B) BLI sensorgram showing binding of tralokinumab to IL4. Tralokinumab was loaded onto an AHC (anti-human capture) sensor and binding was measured with 100 nM recombinant IL4-Fc dimer antigen in solution.

(C) Ociperlimab shows binding to its target TIGIT (blue) and two off-targets, NECTIN4 and SGCA (red).

(D) Comparison of reported ociperlimab epitope residues (based on PDB 8JEL) on TIGIT versus NECTIN4. Six (red) of 15 residues are conserved in NECTIN4 including a histidine matched to H76 (blue), which mediates pH dependent binding to TIGIT. Residue numbering is per Uniprot, and the amino acid lineups for the respective protein pairs are based on a structural alignment returned by the TM-align webserver (https://zhanggroup.org/TM-align/).

(E) BLI sensorgrams showing binding of ociperlimab to a NECTIN4-Fc dimer (top) or NECTIN4 monomer (bottom) at either pH 7.4 or pH 6.0. Ociperlimab displays enhanced binding at pH 6.0. R = response.

examined the impact of otelixizumab on its off-target interaction with interferon gamma receptor I (IFNGR1). As expected, a negative control antibody did not inhibit binding of IFNGR1 to its ligand IFNG (Figure S4A). Similarly, pre-binding otelixizumab to IFNGR1 did not block binding of IFNG, indicating that otelixizumab binds to an epitope distinct from the IFNGR1:IFNG interface (Figure S4B).

Epitope mapping of the tanezumab:TSLP interface

Given the relevance of TSLP as a therapeutic target and the unexpected observation that tanezumab can inhibit its binding to its receptor TSLPR, we sought to define the tanezumab epitope on TSLP. We performed yeast surface display epitope mapping,[28] which we have previously used to characterize binding sites of SARS-CoV-2 antibodies.[11] We constructed a random mutagenesis library of yeast-displayed TSLP variants which was subjected to selection for loss of binding to tanezumab (Figure 3E). Sorted TSLP variants were sequenced to identify mutations that abrogated binding to tanezumab. In total, 246 mutations were identified, with the most highly repeated mutations occurring at positions K40, R72, R149, R150, N152, and R153 (Figure 3F). To assess the impact of the mutations, we performed binding of tanezumab and TSLPR to all identified TSLP variants displayed on yeast. Individual clone testing showed that mutations at 10 positions resulted in significant loss of binding between TSLP and tanezumab (<20% of binding to wild-type TSLP) (Figure 3G). As expected, TSLP variants with mutations in TSLP-TSLPR binding interface[16,17] also reduced binding to TSLPR (Figure 3G). Although the TSLP mutations that reduce or ablate tanezumab binding are discontinuous in sequence space, they cluster to form a structural binding footprint that overlaps with the binding site of TSLPR, thereby explaining the observed competition (Figure 3H). In summary, the TSLP epitope recognized by tanezumab is partially shared and overlaps with the binding sites for both tezepelumab and TSLPR.

Tanezumab specificity engineering to remove off-target TSLP binding

Our observation that single mutations in TSLP can ablate binding to tanezumab suggested that the same effect could be achieved through minimal engineering of the antibody paratope. To examine this, we performed directed evolution engineering of tanezumab to remove off-target binding to while maintaining or improving affinity to its target antigen NGF. To minimize

Please cite this article in press as: Dai et al., Off-target reactivity in clinical monoclonal antibodies, Structure (2026), https://doi.org/10.1016/j.str.2026.02.012

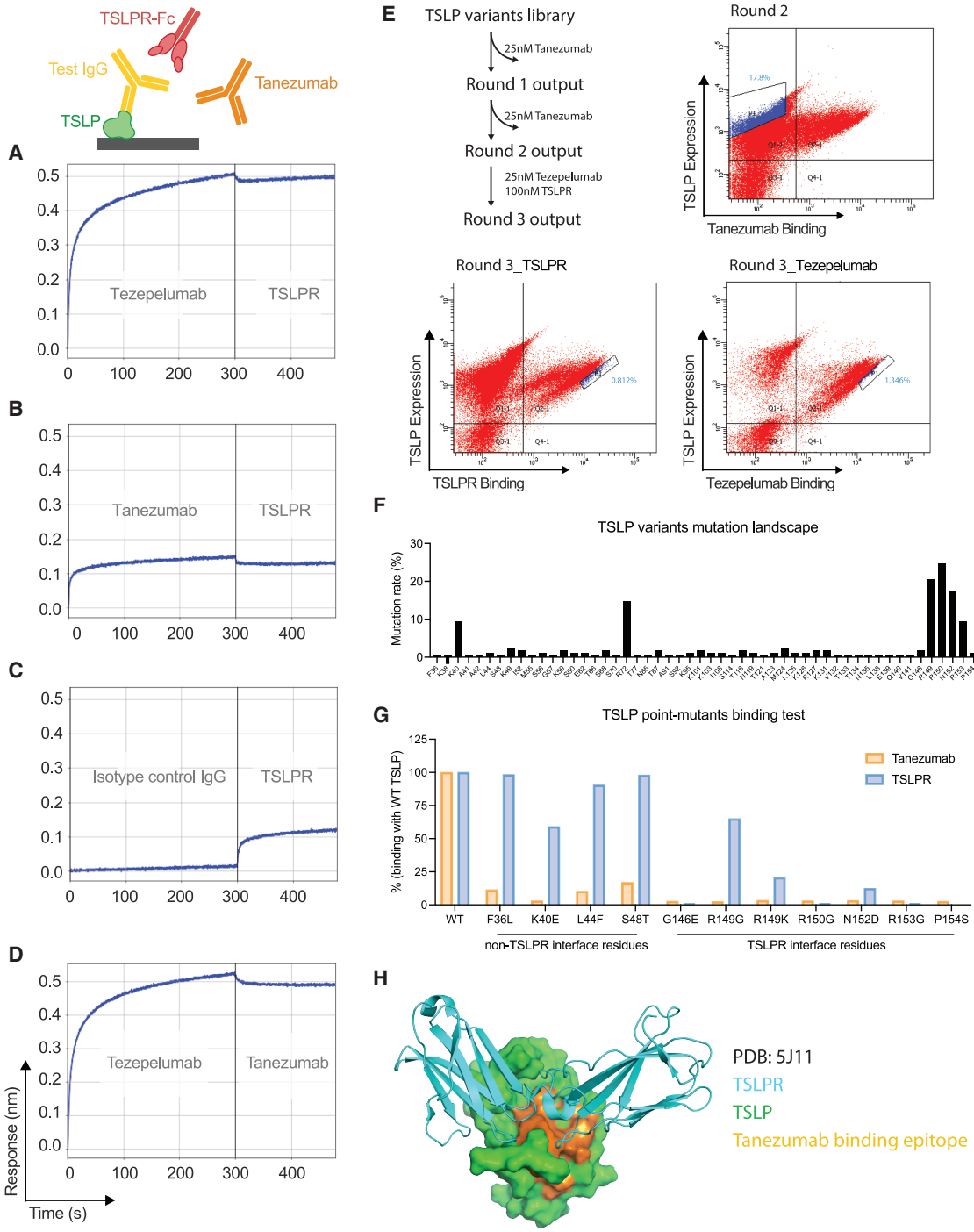

Figure 3. Biophysical characterization of the off-target reactivity of tanezumab to TSLP

(A–C) Test IgG binding to immobilized TSLP is measured in the first step (0–300 s) and soluble TSLPR binding to TSLP is measured in the second step (300–500 s). (A) Tezepelumab binds to immobilized TSLP and blocks subsequent TSLPR binding. (B) Tanezumab binds to immobilized TSLP and blocks TSLPR binding. (C) An isotype negative control IgG does not bind to immobilized TSLP or inhibit TLSPR binding to TSLP.

(D) Tezepelumab binding to TSLP blocks subsequent tanezumab binding.

(E) Selection strategy and FACS plots depicting selection to isolate TSLP variants without tanezumab reactivity while still bind to TSLPR and Tezepelumab.

(F) Mutational analysis of TSLP variants derived from tanezumab epitope mapping selections. Sequencing of TSLP variants from the tanezumab negative selection output revealed 246 unique TSLP mutations across 52 positions. The most highly enriched sites of mutation were at K40, R72, R149, R150, N152, and R153.

(G) Point mutants were tested for binding to tanezumab and TSLPR to determine the loss in binding as compared to wild-type TSLP.

(legend continued on next page)

Please cite this article in press as: Dai et al., Off-target reactivity in clinical monoclonal antibodies, Structure (2026), https://doi.org/10.1016/j.str.2026.02.012

mutational load, separate heavy and light chain libraries were constructed with zero or one mutation per CDR and not more than three mutations per chain. The libraries were subjected to toggled positive and negative binding selection with the target and off-target antigen, respectively (Figures 4A and 4B). From the terminal selection round, all IgG clones with unique sequences were produced in yeast and screened for antigen binding. Based on the screening results, two variants derived from tanezumab (Tv1, Tv2) were selected for production as IgG in CHO cells and tested for antigen binding, non-specific polyreactivity, hydrophobicity, and thermostability. The tanezumab variants Tv1 and Tv2 both showed improved monovalent affinity to NGF (Figure 4C), but no detectable binding to TSLP (Figure 4D). Beyond the improved specificity, the engineered variants showed comparable or improved polyreactivity, hydrophobicity, and Fab melting temperature relative to tanezumab (Table 2). Notably, Tv1 and Tv2 both contain only a single CDR mutation in the LC CDR1 or HC CDR2, respectively (Table 2). Minimal engineering was required to ablate the identified off-target antigen reactivity without negatively affecting target antigen binding or introducing undesirable developability properties as evaluated in our three assays.

Although the identified variants of tanezumab no longer bound TSLP, it is possible that the CDR point mutations could introduce novel off-target specificities. To test this, we screened Tv1 and Tv2 in the REAP assay. As expected, the antibody variants were not found to interact with TSLP and no new off-target binding reactivities were identified, indicating that the CDR mutations responsible for removing the off-target binding did not generate any new specificity (Figure 4E). In summary, a minimalist CDR diversification strategy coupled with selection for the desired binding properties yielded variants with improved specificity profiles.

DISCUSSION

Our systematic profiling of 174 clinical-stage and FDA-approved antibodies reveals a striking finding: 28% of tested antibodies exhibited off-target binding to other human proteins. This high prevalence of off-target reactivity in antibodies deemed suitable for clinical testing challenges fundamental assumptions about therapeutic antibody specificity. While these off-target interactions may not have manifested as clinical toxicities for conventional antibodies—possibly due to insufficient affinity, restricted tissue expression, or non-critical epitopes—they highlight that current development paradigms may be inadequate for ensuring true therapeutic specificity. This is particularly concerning for next-generation modalities that amplify antibody binding into potent effector functions. T cell redirecting therapies (TCEs and CAR-T cells) transform even weak off-target binding into potentially lethal cytotoxic responses against healthy tissues. Similarly, antibody-drug conjugates risk delivering cytotoxic payloads to unintended cells, though internalization requirements may provide some protection. As the field advances toward increasingly potent antibody-based modalities, comprehensive specificity profiling becomes paramount for patient safety.

Defining the specificity properties of an antibody is challenging as the intermolecular interactions (e.g., electrostatic, hydrophobic, etc.) that underlie specific and non-specific binding are shared. This raises the question as to whether screens such as REAP report on specific interactions, non-specific "sticky" reactivity, or both. To that end, while antibodies with multiple REAP off-targets showed elevated median PSR scores (Figure 1F), important exceptions demonstrate that REAP and PSR measure distinct properties. Notably, otilimab exhibited high PSR reactivity (0.52) but no REAP off-targets, while tanezumab showed specific, engineerable off-target binding despite low PSR scores (0.17). These results indicate that REAP generally identifies specific oligoreactive interactions rather than general "stickiness," though high PSR scores should prompt careful evaluation of whether identified REAP hits represent specific or non-specific interactions. Antibodies targeting amyloid-β (Aβ) exemplify this latter category. Six out of seven tested Aβ antibodies exhibited a substantially higher number of REAP identified off target interactions and were enriched among antibodies with elevated PSR scores. This behavior potentially reflects the intrinsic biochemical properties of the amyloid beta peptide, which is amphipathic and conformationally heterogeneous, such that antibodies developed to recognize amyloid beta may inherently tolerate broader electrostatic and hydrophobic interactions. In this context, the apparent polyreactivity of Aβ antibodies likely reflects a combination of target driven binding permissiveness and elevated promiscuity.

The molecular basis of oligospecificity appears to arise through two mechanisms. First, structural homology between targets enables cross-reactivity, as seen with tralokinumab binding both IL13 and IL4, and ociperlimab recognizing both TIGIT and NECTIN4 through partially conserved epitopes.[29,30] More concerning is epitope mimicry in unrelated proteins, exemplified by tanezumab's recognition of an electropositive patch on TSLP that overlaps with functionally critical receptor binding sites. The predominance of charged residues in this interface suggests electrostatic complementarity as a driver of oligospecificity. Notably, off-target epitopes often occur at biologically relevant interfaces; tanezumab competes with TSLPR for TSLP binding, while camrelizumab modulates VEGFR2 signaling through its off-target interaction.[10] These observations suggest that oligospecific binding is not random but may preferentially occur at protein-protein interfaces that have evolved for molecular recognition.

The unpredictability of oligospecific interactions has particular relevance in the era of AI-powered drug design. While computational tools have shown remarkable promise in designing proteins with desired affinity and stability profiles, our results underscore that specificity cannot be reliably predicted from sequence or structure alone. As with other discovery techniques, *de novo* designed antibodies bypass natural immune tolerance mechanisms, potentially increasing the risk of unexpected off-target interactions. The comprehensive REAP profiling data generated here and in future studies could provide crucial training datasets for machine learning models to predict oligospecificity patterns. However, until such predictive models are validated, empirical specificity screening remains essential.

(H) Identified mutations that reduced binding to tanezumab were mapped onto the structure of TSLP in complex with TSLPR (PDB:5J11) to define the tanezumab epitope. TSLPR is shown in cyan as a ribbon drawing, TSLP is represented as space-filling in green and orange (tanezumab epitope positions). The tanezumab epitope overlaps with the binding site of TSLPR.

Please cite this article in press as: Dai et al., Off-target reactivity in clinical monoclonal antibodies, Structure (2026), https://doi.org/10.1016/j.str.2026.02.012

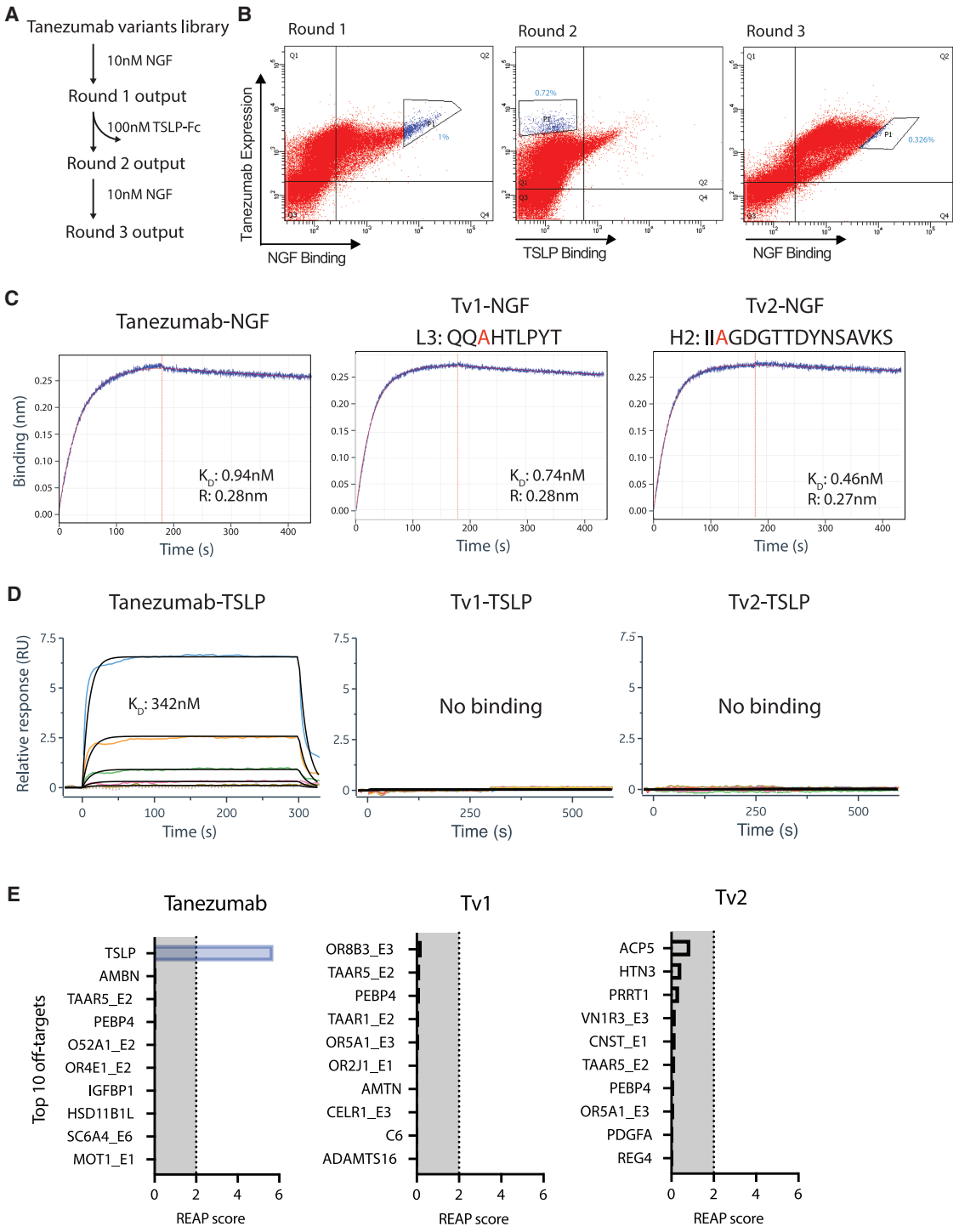

Figure 4. Tanezumab engineering to remove off-target TSLP binding

(A and B) Selection strategy and FACS plots depicting selection to isolate tanezumab variants without TSLP reactivity while retaining binding to NGF.

(C) Tanezumab variants bind with higher affinity to NGF by BLI assay.

(D) Tanezumab variants show no binding to TSLP by Biacore SPR assay.

(E) REAP screen of tanezumab variants confirms absence of off-target antigen reactivity and no introduction of new off-target interactions above the defined REAP threshold.

Please cite this article in press as: Dai et al., Off-target reactivity in clinical monoclonal antibodies, Structure (2026), https://doi.org/10.1016/j.str.2026.02.012

Table 2. Characterization of engineered tanezumab variants

IgG Clone	CDRH2	CDRH3	CDRL3	Target KD [M] (Monovalent)	Off-target KD [M] (Avid)	PSR score (0–1)	HIC RT (min)	Tm (°C)
Tanezumab	IIWGDGTTDYNSAVKS	ARGGYWYATSYYFDY	QQEHTLPYT	9.5E-10	3.4E-07	0.18	11.0	76.0
Tv1	IIWGDGTTDYNSAVKS	ARGGYWYATSYYFDY	QQAHTLPYT	7.4E-10	N.B.	0.00	11.4	88.0
Tv2	IIAGDGTTDYNSAVKS	ARGGYWYATSYYFDY	QQEHTLPYT	4.6E-10	N.B.	0.00	10.6	75.0

Engineered variants of tanezumab retain binding to the target antigen but do not bind the off-target antigen. Monovalent target affinity was determined by biolayer interferometry assay. Avid off-target binding was measured by surface plasmon resonance assay. All variants have comparable or decreased polyreactivity (PSR score) and hydrophobicity (HIC retention time; RT) versus the parent IgG. CDR mutations are highlighted in red. N.B = non-binding. Related to Figure 4.

The risk associated with off-target interactions is challenging to assess and depends on binding affinity, epitope location, and tissue expression of the off-target protein. We demonstrate two practical approaches for managing identified off-targets during antibody development. First, when off-targets are identified in lead candidates, our minimalist engineering strategy of diversifying CDR positions while limiting mutations to 1–2 amino acids successfully ablated off-target binding while maintaining or improving target affinity and developability properties (Table 2). Importantly, these minimal changes did not introduce new off-target reactivities (Figure 4E), suggesting that significant sequence alterations may be required to generate novel specificities. This engineering workflow is generalizable across display platforms and could potentially address multiple off-targets simultaneously. Alternatively, when engineering is not desirable due to time or resource constraints, REAP screening can inform rank-ordering of candidates within a discovery panel. Given that most clinical-stage antibodies showed no detectable off-targets, selecting leads with minimal off-target profiles is a viable strategy when the candidate pool is sufficiently large and diverse. Both approaches, targeted engineering and informed selection, leverage REAP's comprehensive profiling to reduce off-target risk in clinical development.

The identification of off-target reactivities in more than a quarter of clinical-stage antibodies has implications beyond individual drug development programs. Our results strengthen the argument that comprehensive specificity profiling should become part of standard preclinical safety assessments required by regulators, particularly for high-potency modalities. For the biotechnology industry, REAP and similar platforms offer an opportunity to de-risk candidates early in development when engineering solutions remain feasible and cost-effective. The ability to either engineer away off-targets with minimal mutations or select inherently specific candidates from diverse panels provides actionable strategies for improving therapeutic specificity. The tools and approaches demonstrated here provide a foundation for approaching the long-standing goal of highly specific antibody therapeutics without unintended off target binding.

RESOURCE AVAILABILITY

Lead contact

Further information and requests for resources and reagents should be directed to and will be fulfilled by the lead contact, Aaron M. Ring (aaronring@fredhutch.org).

Materials availability

All unique/stable reagents generated in this study are available from the lead contact with a completed materials transfer agreement.

Data and code availability

This study does not report original code. Any additional information required to reanalyze the data reported in this article is available from the lead contact upon request. Source data are provided in this article as Data S1, S2, S3, S4, and S5.

ACKNOWLEDGMENTS

The authors thank all members of the Ring lab and would like to acknowledge the following Adimab employees for their contributions: Cody Williams (figure preparation and layout), Garrett Rappazzo (statistical analysis), Jingfu Zhao and Jonas Spaulding (sample analytics), Melanie Sinclair (antibody production and characterization), Jessica Dawson, Eric Krauland, Juergen Nett, and Max Vásquez (manuscript review). A.M.R. was supported by grants from the Mark Foundation for Cancer Research and the Pew Charitable Trusts and gifts from the Anderson and Bezos Families.

AUTHOR CONTRIBUTIONS

Y.D., J.B., A.S., J.C.G., and A.M.R. designed the study. Y.D., J.B., Z.Z., I.B., A.K.L., A.L., E.M., M.M., L.P., T.S., and C.S. performed experiments. Y.D., J.B., J.R.J., J.D.H., I.B., C.H., A.K. L., A.L., E.M., L.P., A.S., and J.C.G. performed data analysis and data visualization. S.S.Y., K.C.O.'C., M.M., T.S., and C.S. provided reagents. A.S., J.C.G., and A.M.R. supervised the study. Y.D., J.B., S.M.Y., A.S., J.C.G., and A.M.R. wrote the paper with input from all authors.

DECLARATION OF INTERESTS

A.M.R. and Y.D., are inventors of a patent application describing the REAP technology and A.M.R. is a founder and director of Seranova Bio, the commercial licensee of the REAP technology. J.B., I.B., C.H., A.K.L., A.L., E.M., M.M., L.P., T.S., C.S., A.S., and J.C.G. are or were employees of Adimab, LLC.

DECLARATION OF GENERATIVE AI AND AI-ASSISTED TECHNOLOGIES IN THE WRITING PROCESS

During the preparation of this work, the authors used ChatGPT for grammar checking. After using this tool, the authors reviewed and edited the content as needed and take full responsibility for the content of the publication.

STAR★METHODS

Detailed methods are provided in the online version of this paper and include the following:

- KEY RESOURCES TABLE
- EXPERIMENTAL MODEL AND STUDY PARTICIPANT DETAILS
  - Cell lines

SUPPLEMENTAL INFORMATION

Supplemental information can be found online at https://doi.org/10.1016/j.str.2026.02.012.

Received: November 12, 2025
Revised: January 9, 2026
Accepted: February 19, 2026

REFERENCES

1. Crescioli, S., Kaplon, H., Chenoweth, A., Wang, L., Visweswaraiah, J., and Reichert, J.M. (2024). Antibodies to watch in 2024. mAbs *16*, 2297450. https://doi.org/10.1080/19420862.2023.2297450.
2. Jain, T., Sun, T., Durand, S., Hall, A., Houston, N.R., Nett, J.H., Sharkey, B., Bobrowicz, B., Caffry, I., Yu, Y., et al. (2017). Biophysical properties of the clinical-stage antibody landscape. Proc. Natl. Acad. Sci. USA *114*, 944–949. https://doi.org/10.1073/pnas.1616408114.
3. Bailly, M., Mieczkowski, C., Juan, V., Metwally, E., Tomazela, D., Baker, J., Uchida, M., Kofman, E., Raoufi, F., Motlagh, S., et al. (2020). Predicting Antibody Developability Profiles Through Early Stage Discovery Screening. mAbs *12*, 1743053. https://doi.org/10.1080/19420862.2020.1743053.
4. Prigent, J., Jarossay, A., Planchais, C., Eden, C., Dufloo, J., Kök, A., Lorin, V., Vratskikh, O., Couderc, T., Bruel, T., et al. (2018). Conformational Plasticity in Broadly Neutralizing HIV-1 Antibodies Triggers Polyreactivity. Cell Rep. *23*, 2568–2581. https://doi.org/10.1016/j.celrep.2018.04.101.
5. Rabia, L.A., Zhang, Y., Ludwig, S.D., Julian, M.C., and Tessier, P.M. (2018). Net charge of antibody complementarity-determining regions is a key predictor of specificity. Protein Eng. Des. Sel. *31*, 409–418. https://doi.org/10.1093/protein/gzz002.
6. Lecerf, M., Kanyavuz, A., Lacroix-Desmazes, S., and Dimitrov, J.D. (2019). Sequence features of variable region determining physicochemical properties and polyreactivity of therapeutic antibodies. Mol. Immunol. *112*, 338–346. https://doi.org/10.1016/j.molimm.2019.06.012.
7. Van Regenmortel, M.H.V. (2014). Specificity, polyspecificity, and heterospecificity of antibody-antigen recognition. J. Mol. Recognit. *27*, 627–639. https://doi.org/10.1002/jmr.2394.
8. Cunningham, O., Scott, M., Zhou, Z.S., and Finlay, W.J.J. (2021). Polyreactivity and polyspecificity in therapeutic antibody development: risk factors for failure in preclinical and clinical development campaigns. mAbs *13*, 1999195. https://doi.org/10.1080/19420862.2021.1999195.
9. Nemazee, D. (2017). Mechanisms of central tolerance for B cells. Nat. Rev. Immunol. *17*, 281–294. https://doi.org/10.1038/nri.2017.19.
10. Finlay, W.J.J., Coleman, J.E., Edwards, J.S., and Johnson, K.S. (2019). Anti-PD1 'SHR-1210' aberrantly targets pro-angiogenic receptors and this polyspecificity can be ablated by paratope refinement. mAbs *11*, 26–44. https://doi.org/10.1080/19420862.2018.1550321.
11. Rappazzo, C.G., Tse, L.V., Kaku, C.I., Wrapp, D., Sakharkar, M., Huang, D., Deveau, L.M., Yockachonis, T.J., Herbert, A.S., Battles, M.B., et al. (2021). Broad and potent activity against SARS-like viruses by an engineered human monoclonal antibody. Science (New York, N.Y.) *371*, 823–829. https://doi.org/10.1126/science.abf4830.
12. Wec, A.Z., Wrapp, D., Herbert, A.S., Maurer, D.P., Haslwanter, D., Sakharkar, M., Jangra, R.K., Dieterle, M.E., Lilov, A., Huang, D., et al. (2020). Broad neutralization of SARS-related viruses by human monoclonal antibodies. Science (New York, N.Y.) *369*, 731–736. https://doi.org/10.1126/science.abc7424.
13. Vicart, A., Holland, C., Fraser, K., Gervais, F., Aspinall-O'Dea, M., Brown, N., Siddals, K., Greiner, G., Carreira, V., Galbreath, E., et al. (2025). Applications of Cell-Based Protein Array Technology to Preclinical Safety Assessment of Biological Products. Toxicol. Pathol. *53*, 31–44. https://doi.org/10.1177/01926233241311259.
14. Norden, D.M., Navia, C.T., Sullivan, J.T., and Doranz, B.J. (2024). The emergence of cell-based protein arrays to test for polyspecific off-target binding of antibody therapeutics. mAbs *16*, 2393785. https://doi.org/10.1080/19420862.2024.2393785.
15. Wang, E.Y., Dai, Y., Rosen, C.E., Schmitt, M.M., Dong, M.X., Ferré, E.M.N., Liu, F., Yang, Y., González-Hernández, J.A., Meffre, E., et al. (2022). High-throughput identification of autoantibodies that target the human exoproteome. Cell Rep. Methods *2*, 100172. https://doi.org/10.1016/j.crmeth.2022.100172.
16. Marković, I., and Savvides, S.N. (2020). Modulation of Signaling Mediated by TSLP and IL-7 in Inflammation, Autoimmune Diseases, and Cancer. Front. Immunol. *11*, 1557. https://doi.org/10.3389/fimmu.2020.01557.
17. Verstraete, K., Peelman, F., Braun, H., Lopez, J., Van Rompaey, D., Dansercoer, A., Vandenberghe, I., Pauwels, K., Tavernier, J., Lambrecht, B.N., et al. (2017). Structure and antagonism of the receptor complex mediated by human TSLP in allergy and asthma. Nat. Commun. *8*, 14937. https://doi.org/10.1038/ncomms14937.
18. Bumbaca, D., Wong, A., Drake, E., Reyes, A.E., 2nd, Lin, B.C., Stephan, J.P., Desnoyers, L., Shen, B.Q., and Dennis, M.S. (2011). Highly specific off-target binding identified and eliminated during the humanization of an antibody against FGF receptor 4. mAbs *3*, 376–386. https://doi.org/10.4161/mabs.3.4.15786.
19. Xu, Y., Roach, W., Sun, T., Jain, T., Prinz, B., Yu, T.Y., Torrey, J., Thomas, J., Bobrowicz, P., Vásquez, M., et al. (2013). Addressing polyspecificity of antibodies selected from an *in vitro* yeast presentation system: a FACS-based, high-throughput selection and analytical tool. Protein Eng. Des. Sel. *26*, 663–670. https://doi.org/10.1093/protein/gzt047.
20. Shehata, L., Maurer, D.P., Wec, A.Z., Lilov, A., Champney, E., Sun, T., Archambault, K., Burnina, I., Lynaugh, H., Zhi, X., et al. (2019). Affinity Maturation Enhances Antibody Specificity but Compromises Conformational Stability. Cell Rep. *28*, 3300–3308.e4. https://doi.org/10.1016/j.celrep.2019.08.056.
21. Brocker, C., Thompson, D., Matsumoto, A., Nebert, D.W., and Vasiliou, V. (2010). Evolutionary divergence and functions of the human interleukin (IL) gene family. Hum. Genomics *5*, 30–55. https://doi.org/10.1186/1479-7364-5-1-30.
22. Popovic, B., Breed, J., Rees, D.G., Gardener, M.J., Vinall, L.M.K., Kemp, B., Spooner, J., Keen, J., Minter, R., Uddin, F., et al. (2017). Structural Characterisation Reveals Mechanism of IL-13-Neutralising Monoclonal Antibody Tralokinumab as Inhibition of Binding to IL-13Rα1 and IL-13Rα2. J. Mol. Biol. *429*, 208–219. https://doi.org/10.1016/j.jmb.2016.12.005.
23. Sun, J., Zhang, X., Xue, L., Cheng, L., Zhang, J., Chen, X., Shen, Z., Li, K., Wang, L., Huang, C., et al. (2024). Structural insights into the unique pH-responsive characteristics of the anti-TIGIT therapeutic antibody Ociperlimab. Structure (London, England : 1993) *32*, 550–561.e5. https://doi.org/10.1016/j.str.2024.02.009.
24. Harrison, O.J., Vendome, J., Brasch, J., Jin, X., Hong, S., Katsamba, P.S., Ahlsen, G., Troyanovsky, R.B., Troyanovsky, S.M., Honig, B., et al. (2012). Nectin ectodomain structures reveal a canonical adhesive interface. Nat. Struct. Mol. Biol. *19*, 906–915. https://doi.org/10.1038/nsmb.2366.

25. Schnitzer, T.J., Easton, R., Pang, S., Levinson, D.J., Pixton, G., Viktrup, L., Davignon, I., Brown, M.T., West, C.R., and Verburg, K.M. (2019). Effect of Tanezumab on Joint Pain, Physical Function, and Patient Global Assessment of Osteoarthritis Among Patients With Osteoarthritis of the Hip or Knee: A Randomized Clinical Trial. JAMA *322*, 37–48. https://doi.org/10.1001/jama.2019.8044.

26. Menzies-Gow, A., Corren, J., Bourdin, A., Chupp, G., Israel, E., Wechsler, M.E., Brightling, C.E., Griffiths, J.M., Hellqvist, Å., Bowen, K., et al. (2021). Tezepelumab in Adults and Adolescents with Severe, Uncontrolled Asthma. N. Engl. J. Med. *384*, 1800–1809. https://doi.org/10.1056/NEJMoa2034975.

27. Miller, S.A., and St Onge, E. (2011). Otelixizumab: a novel agent for the prevention of type 1 diabetes mellitus. Expert Opin. Biol. Ther. *11*, 1525–1532. https://doi.org/10.1517/14712598.2011.610789.

28. Chao, G., Cochran, J.R., and Wittrup, K.D. (2004). Fine epitope mapping of anti-epidermal growth factor receptor antibodies through random mutagenesis and yeast surface display. J. Mol. Biol. *342*, 539–550. https://doi.org/10.1016/j.jmb.2004.07.053.

29. McCormick, S.M., and Heller, N.M. (2015). Commentary: IL-4 and IL-13 receptors and signaling. Cytokine *75*, 38–50. https://doi.org/10.1016/j.cyto.2015.05.023.

30. Reches, A., Ophir, Y., Stein, N., Kol, I., Isaacson, B., Charpak Amikam, Y., Elnekave, A., Tsukerman, P., Kucan Brlic, P., Lenac, T., et al. (2020). Nectin4 is a novel TIGIT ligand which combines checkpoint inhibition and tumor specificity. J. Immunother. Cancer *8*, e000266. https://doi.org/10.1136/jitc-2019-000266.

31. Liu, C.Y., Ahonen, C.L., Brown, M.E., Zhou, L., Welin, M., Krauland, E.M., Pejchal, R., Widboom, P.F., and Battles, M.B. (2023). Structure-based engineering of a novel CD3ε-targeting antibody for reduced polyreactivity. mAbs *15*, 2189974. https://doi.org/10.1080/19420862.2023.2189974.

32. He, F., Woods, C.E., Trilisky, E., Bower, K.M., Litowski, J.R., Kerwin, B.A., Becker, G.W., Narhi, L.O., and Razinkov, V.I. (2011). Screening of monoclonal antibody formulations based on high-throughput thermostability and viscosity measurements: design of experiment and statistical analysis. J. Pharm. Sci. *100*, 1330–1340. https://doi.org/10.1002/jps.22384.

Please cite this article in press as: Dai et al., Off-target reactivity in clinical monoclonal antibodies, Structure (2026), https://doi.org/10.1016/j.str.2026.02.012

STAR★METHODS

KEY RESOURCES TABLE

REAGENT or RESOURCE	SOURCE	IDENTIFIER
Antibodies		
Bavencio	Evidentic GmbH	#08000471
Imfinzi	Evidentic GmbH	#08000488
Avastin	Evidentic GmbH	#08000005
Cosentyx	Evidentic GmbH	#08000330
Cyramza	Evidentic GmbH	#08000293
Darzalex	Evidentic GmbH	#08000011
Enbrel	Evidentic GmbH	#08000057
Erbitux	Evidentic GmbH	#08000034
Gazyvaro	Evidentic GmbH	#08000100
Herceptin	Evidentic GmbH	#08000353
Humira	Evidentic GmbH	#08000028
Keytruda	Evidentic GmbH	#08000264
Mabthera	Evidentic GmbH	#08000318
Opdivo	Evidentic GmbH	#08000092
Prolia	Evidentic GmbH	#08000040
Remicade	Evidentic GmbH	#08000086
RoActemra	Evidentic GmbH	#08000347
Simponi	Evidentic GmbH	#08000063
Synagis	Evidentic GmbH	#08000258
Tanezumab	Thermo Fisher	MA5-41831; RRID: AB_2910974
Otelixizumab	Thermo Fisher	MA5-41836; RRID: AB_2910979
Fletikumab	Thermo Fisher	MA5-42014; RRID: AB_2911157
Carlumab	Thermo Fisher	MA5-41926; RRID: AB_2911069
Enokizumab	Thermo Fisher	MA5-41928; RRID: AB_2911071
Tigatuzumab	Thermo Fisher	MA5-41835; RRID: AB_2910978
Fezakinumab	Thermo Fisher	MA5-41905; RRID: AB_2911048
Galiximab	Thermo Fisher	MA5-41774; RRID: AB_2910917
Olokizumab	Thermo Fisher	MA5-41921; RRID: AB_2911064
Lumiliximab	Thermo Fisher	MA5-41778; RRID: AB_2910921
Codrituzumab	Thermo Fisher	MA5-42002; RRID: AB_2911145
Lebrikizumab	Thermo Fisher	MA5-41906; RRID: AB_2911049
Sarilumab	Thermo Fisher	MA5-41953; RRID: AB_2911096
Bimagrumab	Thermo Fisher	MA5-41992; RRID: AB_2911135
Gevokizumab	Thermo Fisher	MA5-41730; RRID: AB_2910873
Other drug product IgG samples, see Data S2	Twist	N/A
anti-human LC-FITC	Southern Biotech	#2062-02
anti-HA-APC	Biolegend	#901524; RRID: AB_2734657
anti-hIgG R-PE	Southern Biotech	#0151K-09
Biological samples		
Human TSLP	ACROBiosystems	#TSP-H52Hb
Human IFNGR1	ACROBiosystems	#IF1-H5223
Human TFF3	R&D Systems	#8294-TF-050
Human CA12	R&D Systems	#2190-CA-010
Human CD160	ACROBiosystems	#BY5-H5229

(*Continued on next page*)

Please cite this article in press as: Dai et al., Off-target reactivity in clinical monoclonal antibodies, Structure (2026), https://doi.org/10.1016/j.str.2026.02.012

Continued

REAGENT or RESOURCE	SOURCE	IDENTIFIER
Human IL4	ACROBiosystems	#IL4-H5253
Human NECTIN4	ACROBiosystems	#NE4-H5255
Human IFNA8	R&D Systems	#11018-IF-050
Human NGF	R&D Systems	#256-GF-100/CF
Human TSLPR	R&D Systems	#981-TR-050
Human IFNγ	R&D Systems	#CAA31639, #285-IF-100/CF
Human TDGF1-HIS	This study	N/A
Human TSLP-Fc	This study	N/A
Human IFNGR1-Fc	This study	N/A
Human CD3 epsilon-delta (εδ) heterodimer antigen	This study	N/A
Chemicals, peptides, and recombinant proteins		
Polyethylenimine (PEI)	PEIpro	Polyplus #115-100
QuantTag biotin kit	Vector Laboratories	#BDK-200
Expi293 media	Thermo Fisher	#A14635
Ni-NTA agarose	Qiagen	#30210
Anti-Clumping Supplement	Irvine Scientific	#91150
Sephadex G-25 resin	Sigma-Aldrich	#G2580
μMACS Protein G beads	Miltenyi Biotec	#130-071-101
Zymoprep-96 Yeast Plasmid Miniprep kits	Zymo Research	#D2007
MiSeq Reagent Kit v3 (150-cycle)	illumina	#MS-102-3001
Streptavidin 633	Thermo Fisher Scientific	#S21375
propidium iodide	Sigma-Aldrich	#11348639001
GoTaq	Promega	#M7133
8-oxo-dGTP	Jena Bioscience	#NU1117L
dPTP	Jena Bioscience	#NU-1119L
Gel and PCR Clean-Up Kit	Macherey-Nagel	#740609.250
NHS-LC-Biotin	Pierce	21336
Oligonucleotides		
Primer: bc1-TTGTTAATATACCTCTATACTTTAA CGTCAAGGAGAAAAAACCCCGGATC	This study	N/A
Primer: bc2-CTGCATCCTTTAGTGAG GGTTGAANNNNNNNNNNNNNNNTTCGA TCCGGGGTTTTTTCTCCTTG	This study	N/A
Primer: bc3-TTCAACCCTCACTAAAGG ATGCAGTTACTTCGCTGTTTTTCAATA TTTTCTGTTATTGC	This study	N/A
Primer: bc4-TGCTAAAACGCTAGCAA TAACAGAAAATATTGAAAAACAGCG	This study	N/A
Primer:159_DIF2-TCGTCGGCAGCG TCAGATGTGTATAAGAGACAGNNNNN NNNNNGAGAAAAAACCCCGGATCG	This study	N/A
Primer: 159_DIR2-GTCTCGTGGGCTCGGAGA TGTGTATAAGAGACAGNNNNNNNNNNAC GCTAGCAATAACAGAAAATATTG	This study	N/A
Other		
Mono Q anion exchange column	Cytiva Life Sciences	#17516701
Superdex200 size exclusion chromatography column	Cytiva Life Sciences	#28989335
AHC (anti-human capture) sensor	Sartorius	#18–5064
streptavidin sensor	Sartorius	#18-5021
Multi-96 Columns	Miltenyi Biotec	#130-092-444
MultiMACS M96 Separator	Miltenyi Biotec	#130-091-937
PyMol	Schrödinger, LLC	N/A

Please cite this article in press as: Dai et al., Off-target reactivity in clinical monoclonal antibodies, Structure (2026), https://doi.org/10.1016/j.str.2026.02.012

EXPERIMENTAL MODEL AND STUDY PARTICIPANT DETAILS

Cell lines

Chinese Hamster Ovary (CHO) cells: used for IgG production and PSR assay.
HEK293 cells: used for CD3 epsilon-delta Fc-fusion protein production.
Expi293 cells (Thermo Fisher, #A14635): used for TDGF1 protein expression.

Microbe strains

Saccharomyces cerevisiae: used for yeast surface display (REAP screening, antibody selections, epitope mapping) and Fc-fusion protein production.

METHOD DETAILS

IgG reagents

Drug product IgG samples were sourced from Evidentic, GmbH (Berlin, Germany). The remaining clinical-stage antibodies were cloned as human IgG1 and produced by Twist Bioscience (South San Francisco, CA) or obtained from ThermoFisher (tanezumab, MA5-41831; otelixizumab, MA5-41836; fletikumab, MA5-42014; carlumab, MA5-41926; enokizumab, MA5-41928; tigatuzumab, MA5-41835; fezakinumab, MA5-41905; galiximab, MA5-41774; olokizumab, MA5-41921; lumiliximab, MA5-41778; codrituzumab, MA5-42002; lebrikizumab, MA5-41906; sarilumab, MA5-41953; bimagrumab, MA5-41992; gevokizumab, MA5-41730) (Data S2). Engineered tanezumab and otelixizumab variants were cloned as human IgG1 and produced by transient transfection in Chinese hamster ovary suspension cells. Two plasmids encoding the full heavy and light chains were transiently co-transfected at a 1:1 ratio using polyethylenimine (PEI) transfection reagent (PEIpro, Polyplus #115-100). Transfected cells were cultured in a 37°C incubator with 8% CO2, shaking at 130 rpm. After 24 h, they were transferred to conditions of 32°C in a 5% CO2 incubator, still shaking at 130 rpm. During this period, they were given mammalian production feed medium (at 2% v/v) supplemented with valproic acid (at 1 mM) and anti-clumping reagent (Irvine Scientific #91150). At 4 days and 7 days of growth, the cells received the mammalian production feed medium again (at 4% v/v). After 9 days, the supernatant was collected and purified by protein A affinity chromatography. The column was equilibrated and washed with PBS, and bound protein was eluted with 0.1 M glycine (pH 3.0). Eluted fractions were immediately neutralized 9:1 with 1 M Tris-HCl (pH 8.0).

Antigen reagents

Human TSLP for BLI and SPR binding assays was obtained from Acro Biosystems (Acro, #TSP-H52Hb). Human IFNGR1 for BLI and SPR binding assays was obtained from Acro (#IF1-H5223). Human TFF3 was obtained from R&D (#8294-TF-050). Human CA12 was obtained from R&D (#2190-CA-010). Human CD160 was obtained from Acro (#BY5-H5229). Human IL4 was obtained from Acro (#IL4-H5253). Human NECTIN4 was obtained from Acro (#NE4-H5255). Human IFNA8 was obtained from R&D (#11018-IF-050) and then biotinylated through primary amine coupling using a QuantTag biotin kit (Vector Laboratories, #BDK-200). Human NGF for use in selections and IgG binding was obtained from R&D (#256-GF-100/CF). Human TSLPR (CRLF2) (accession #Q9HC73) for use in epitope mapping selections and BLI competition assays was obtained from R&D (#981-TR-050). Human IFNγ was obtained from R&D (accession #CAA31639, #285-IF-100/CF). The human TDGF1 protein (L31-D150) with a C-terminal 8xHIS-tag was cloned into a mammalian expression vector and expressed in the Expi293 system (Thermo Fisher, #A14635), and purified with Ni-NTA Agarose (Qiagen, #30210).

TSLP and IFNGR1 fusion proteins used in specificity engineering selections were generated by fusion of the mature TSLP protein (Tyr29-Gln159) or ectodomain of IFNGR1 (Glu18-Gly245) to an aglycosylated (N297A) human IgG1. Each protein was tagged with an N-terminal HA epitope and G_4S linker; a second G_4S linker was introduced between the antigen and the Fc domain. Both fusion proteins were produced in S. cerevisiae, as previously described for IgGs.[12] Briefly, yeast cultures were incubated in 24-well plates at 30°C, 80% relative humidity with shaking in Infors Multitron shakers. After 6 days of growth, the culture supernatants were harvested by centrifugation, and Fc fusion proteins were purified by protein A affinity chromatography. Bound proteins were eluted with 200 mM acetic acid with 50 mM NaCl (pH 3.5) and neutralized with 1/8 (v/v) 2 M HEPES (pH 9.0). Human CD3 epsilon-delta (εδ) heterodimer antigen used in specificity selections and IgG binding was produced as an Fc-fusion with a C-terminal HIS-tag via transient transfection in HEK293 cell lines as previously described.[31] Briefly, the extracellular domains of human CD3 epsilon (accession #P07766, AA Met1-Asp126) and human CD3 delta (accession #P04234. AA Met1-Asp100) were inserted into plasmids containing a human IgG1 Fc domain. After co-transfection with PEIpro (Polyplus #115–100), the cells were grown in an incubator at 37°C and 8% CO2, while shaking at 110 rpm. After six days, the supernatant was harvested and purified by a Nickel Sepharose column equilibrated in PBS, with bound protein eluted using PBS containing 250 mM imidazole. Following buffer exchange into PBS with a Sephadex G-25 resin (Sigma-Aldrich, #G2580), the proteins were further purified with a Mono Q anion exchange column (Cytiva Life Sciences, #17516701) using 20 mM Tris (pH 8.0) and a 0–500 mM NaCl gradient, and a Superdex200 size exclusion chromatography column (Cytiva Life Sciences, #28989335) in PBS.

Please cite this article in press as: Dai et al., Off-target reactivity in clinical monoclonal antibodies, Structure (2026), https://doi.org/10.1016/j.str.2026.02.012

REAP assay

REAP was performed as previously described[15] and the updated library was used in this study (Data S1). In brief, 5 μg mAb was incubated with 10 OD induced library yeast in 100 μL PBE (PBS with 0.5% BSA and 0.5 mM EDTA) with shaking for 1 h at 4°C, followed by 30 min incubation with 1:20 μMACS Protein G beads (Miltenyi Biotec) in 100 μL PBE with shaking at 4°C. MicroBeads captured yeast was positively selected by Multi-96 Columns (Miltenyi Biotec) placed in MultiMACS M96 Separator (Miltenyi Biotec). Selected yeast were recovered in 1 mL SDO −Ura at 30°C for 24 h. DNA was extracted from yeast libraries using Zymoprep-96 Yeast Plasmid Miniprep kits (Zymo Research). Purified plasmids were amplified and indexed (2 rounds Phusion PCR, 24 cycles/round), gel purified, and sequenced on an Illumina MiSeq Instrument with MiSeq Reagent Kit v3 (150-cycle). REAP score was calculated as previously described.[15] In brief, it is the adjusted Log2 fold change between the frequency of each protein in pre- and post-selection library and (Log2 fold change $\geq$ 2) is used as a threshold for hits identification.

Specificity engineering of tanezumab and otelixizumab

Tanezumab diversification libraries were generated using an NNK oligo-based approach. For each of the six CDRs, CDR-encoding oligos (IDT, Coralville, IA) were generated with single amino acid mutations introduced by an NNK codon across all CDR positions (one mutation per oligo). Full length variable heavy (VH) and light (VL) genes were constructed by overlap extension PCR of the oligos encoding the diversified CDRs and oligos encoding fixed framework regions. The VH and VL genes were then recombined in *S.cerevisiae* with digested backbone heavy chain and light chain plasmid vectors by electroporation to create yeast display libraries with a diversity of $\sim$1x10^6, as previously described.[11] The diversified VHs and VLs were paired with the parental, non-diversified VL or VH, respectively.

The four tanezumab diversity libraries underwent at least three rounds of sorting by flow cytometry. In the initial round, a positive selection was performed whereby antibody expressing yeast were incubated with the 10nM biotinylated NGF. After incubation, yeast were washed with PBSF (1x PBS, 0.1% [w/v] BSA) and stained with anti-human LC-FITC (Southern Biotech, #2062-02), Streptavidin 633 (Thermo Fisher Scientific, #S21375), and propidium iodide (Sigma-Aldrich, #11348639001). After staining, yeast were washed with PBSF and and analyzed on a BD FACS Aria II (Becton Dickerson). Yeast cells displaying maintained target antigen binding were sorted and propagated. In the second selection round, a negative selection was performed whereby yeast was labeled with 100nM biotinylated TSLP-Fc. Washing and secondary antibody labeling was performed as described for the first selection round. Yeast clones exhibiting no or decreased binding to the off-target antigen were sorted and propagated. In the third selection round, a positive selection was performed whereby yeast were incubated with 10nM biotinylated NGF at the same incubation conditions as is the initial round. Yeast clones exhibiting target binding equivalent to or better than the parental IgG were sorted. The tanezumab libraries underwent a fourth round of positive sorting whereby the yeast was incubated with biotinylated TSLP at 1 nM and the yeast clones exhibiting the best binding were sorted. The selected yeast outputs from the terminal rounds were plated on agar growth media and single colonies were picked for VH and VL Sanger sequencing.

Tanezumab TSLP epitope mapping

For tanezumab epitope mapping, an error-prone PCR mutagenesis library for TSLP was constructed by the addition of degenerate nucleotides to a PCR amplification reaction of a template gBlock (IDT) encoding the TSLP gene fused to an N-terminal HA epitope tag. PCR was performed with GoTaq (Promega, #M7133) according the the manufacturer's recommendations with the addition of 8-oxo-dGTP (Jena Bioscience, #NU1117L) and dPTP (Jena Bioscience, #NU-1119L) at a final concentration of 1 μM each. The PCR amplicons were purified (Nucleospin Gel and PCR Clean-Up Kit, Macherey-Nagel, #740609.250) and cloned into an Aga2-fusion yeast display vector by electroporation and homologous recombination to generate a mutagenized TSLP yeast display library as previously described.[11] For the first round of cell sorting by flow cytometry, the yeast library was incubated with 25 nM tanezumab IgG. Cells were washed with PBSF and stained with anti-HA-APC (Biolegend, #901524), anti-hIgG R-PE (Southern Biotech, #0151K-09), and propidium iodide (Sigma-Aldrich, #11348639001). The cells were washed with PBSF and sorted on a BD FACS Aria II (Becton Dickerson). Yeast cells with decreased or no binding to tanezumab compared to a wild-type TSLP clone were sorted and propagated. An identical second round of selection was performed to further enrich for TSLP mutants with diminished tanezumab binding. In the terminal round of sorting, a positive selection was performed whereby the yeast were labeled with either the anti-TSLP IgG tezepelumab at 25 nM, or TSLPR at 100 nM. Yeast were sorted that exhibited binding to either tezepelumab or TSLPR. Sorted cells were Sanger sequenced. Unique TSLP mutants displayed on yeast were tested for binding to tanezumab, tezepelumab, and TSLPR in solution at 100 nM by flow cytometric analysis on a BD FACS Canto II (BD Biosciences). The binding signal was calculated as a percentage of the binding signal (MFI) of the native TSLP protein. Mapping of the identified epitope positions on the existing TSLP/TSLPR co-crystal structure (PDB 5J11) was performed using PyMol (The PyMOL Molecular Graphics System, Version 3.0 Schrödinger, LLC).

Antigen binding kinetics by biolayer interferometry

The Octet HTX system from Sartorius was employed to assess apparent IgG binding affinities to the described recombinant antigens, following established procedures. All reagents were prepared in PBSF (PBS with 0.1% (w/v) BSA), and the binding steps were executed with an orbital shaking speed of 1000 rpm at 25°C. Binding was measured with either IgG or antigen on the sensor. To evaluate IgG binding to the recombinant antigen in solution, the antibody was captured onto an AHC (anti-human capture) sensor (Sartorius, #18–5064) in a 100 nM solution, resulting in a sensor loading of approximately 0.6–1.2 nm. After a brief 60-s baseline step in

Please cite this article in press as: Dai et al., Off-target reactivity in clinical monoclonal antibodies, Structure (2026), https://doi.org/10.1016/j.str.2026.02.012

PBSF, the association of the antigen (at a concentration of 100 nM) was monitored for 180 s. Subsequently, the sensors were immersed in buffer for another 180 s to observe the dissociation of the antigen. For measurements with antigen on sensor and IgG in solution, biotinylated antigen was captured on a streptavidin sensor (Sartorius, #18–5021) and association and dissociation of IgG in solution (at a concentration of 100 nM) was monitored. Response values obtained were analyzed using the Octet BLI Analysis Software version 12.2.13.5. For response values exceeding 0.1 nm, kinetic association and dissociation rate constants (kon and koff) were determined for each curve by fitting to a 1:1 binding model. The dissociation constants (KD values) were calculated as the ratio of koff/kon.

Tanezumab and otelixizumab competitive binding experiments by biolayer-interferometry

Competition of TSLPR binding to TSLP by tanezumab and tezepelumab was assessed using an an Octet HTX (Sartorius) instrument. All protein reagents were diluted in PBSF. Streptavidin (SA) sensors were loaded with 100 nM biotinylated monomeric TSLP protein. Sensor tips were then equilibrated in PBSF for 30 min. TSLP loaded sensors were transferred to wells containing tanezumab or tezepelumab IgG at 1μM (300 s) and then transferred to wells containing TSLPR-Fc fusion protein at 300 nM (180 s). Competition of tezepelumab with tanezumab for binding to TSLP was assessed in a similar manner. After TSLP loading onto an SA sensor the sensor was transferred to wells containing tezepelumab at 1μM (300 s) followed by transfer to wells containing tanezumab at 300 nM (180 s). Competition of IFNɣ binding to IFNGR1 was assessed by first loading biotinylated monomeric IFNGR1 at 100 nM on SA sensors followed by equilibration in PBSF for 30 min. Next, sensors were transferred to wells containing either otelixizumab or negative control IgG at 300 nM (220 s) and then transferred to wells containing IFNɣ at 300 nM (280 s). Data were aligned by x- and y axes using the Octet BLI analysis software version 12.2.13.5.

PSR assay

The polyspecificity reagent (PSR) assay was conducted following a previously established protocol.[19] In brief, soluble and membrane-enriched fractions were obtained from CHO cells and subsequently biotinylated using NHS-LC-Biotin (Pierce, 21336; Thermo Fisher). The biotinylated reagent was then incubated with IgG molecules displayed on the surface of yeast cells. After thorough washing, the samples were labeled with a secondary mix containing Extravidin-R-PE, anti-human LC-FITC, and propidium iodide. The resulting samples were analyzed using a FACSCanto flow cytometer (BD Biosciences). Median fluorescence intensity (MFI) in the R-PE channel was quantified to evaluate non-specific binding. MFI values were normalized and converted to a score ranging from 0 to 1, based on comparison with three reference antibodies that exhibited low, medium, and high PSR MFI values. A score of 0 indicates no binding, while a score of 1 signifies high PSR binding.

HIC assay

Hydrophobic Interaction Chromatography (HIC) was conducted following an established protocol.[2] In summary, 5 μg of IgG (at a concentration of 1 mg/mL) was mixed with mobile phase A solution containing 1.8 M ammonium sulfate and 0.1 M sodium phosphate at pH 6.5. This combination achieved a final ammonium sulfate concentration of 1 M. The samples were then subjected to analysis using a Sepax Proteomix HIC butyl-NP5 column. During the analysis, a linear gradient of mobile phase A and mobile phase B solution (containing 0.1 M sodium phosphate at pH 6.5) was applied over 20 min, with a flow rate of 1 mL/min. UV absorbance was monitored at 280 nm.

Thermostability analysis

Fab melting temperatures of tanezumab, otelixizumab, and associated variants were measured using a CFX96 Real-Time System (BioRad), based on a previously described protocol.[32] Briefly, 20 μL of a 1 mg/mL sample was mixed with 10 μL of 20 × SYPRO orange. The plate was scanned from 40°C to 95°C at a rate of 0.5°C/2 min. The Fab Tm was assigned using the first derivative of the raw data obtained from the BioRad analysis software.

QUANTIFICATION AND STATISTICAL ANALYSIS

Statistical analyses were performed using GraphPad Prism (V10). For comparing PSR scores across antibody groups binned by number of off-targets, we used two-sided Kruskal-Wallis tests with Dunn's correction for multiple comparisons (Figure 1F). Statistical significance thresholds, sample sizes, and other experimental details are provided in the corresponding figure legends and STAR Methods section.

Structure, Volume *34*

Supplemental Information

Off-target reactivity in clinical monoclonal antibodies

Yile Dai, Joseph Brouillard, Jillian R. Jaycox, Sung M. Yeon, John D. Huck, Soumya S. Yandamuri, Zhe Zhong, Kevin C. O'Connor, Irina Burnina, Cameron Henkel, Allie K. LeMay, Asparouh Lilov, Elizabeth McGurk, Morgan Morrill, Liz Parker, Tricia Sackett, Chanita Sandberg, Arvind Sivasubramanian, James C. Geoghegan, and Aaron M. Ring

Supplementary figures

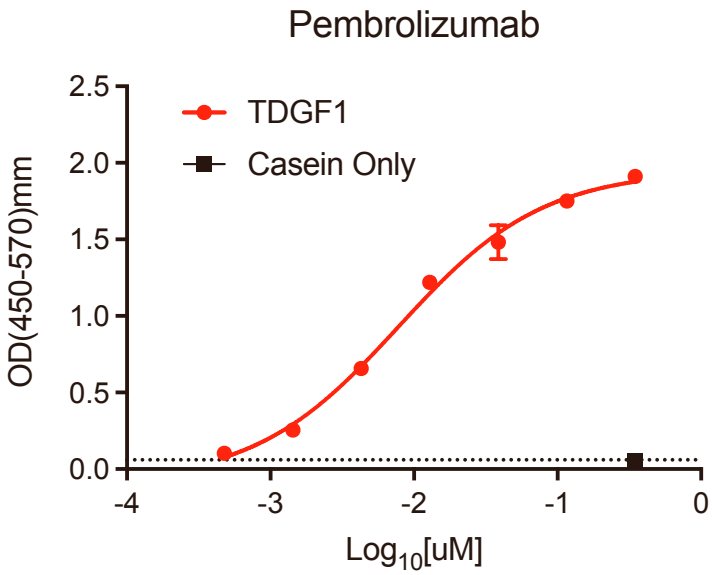

Figure S1. **Validation of Pembrolizumab binding to TDGF1. Related to Figure 1b.** Pembrolizumab binds in a dose-dependent manner to soluble TDGF1 (gene ID:CRIPTO) as measured by enzyme linked immunosorbent assay. Plate wells were coated with TDGF1 or casein, followed by incubation with varying concentrations of pembrolizumab. Binding was detected using an anti-human Fc-HRP secondary antibody and enhanced chemiluminescence readout. OD = optical density. Data are presented as mean ± SD of two independent replicates (n=2).

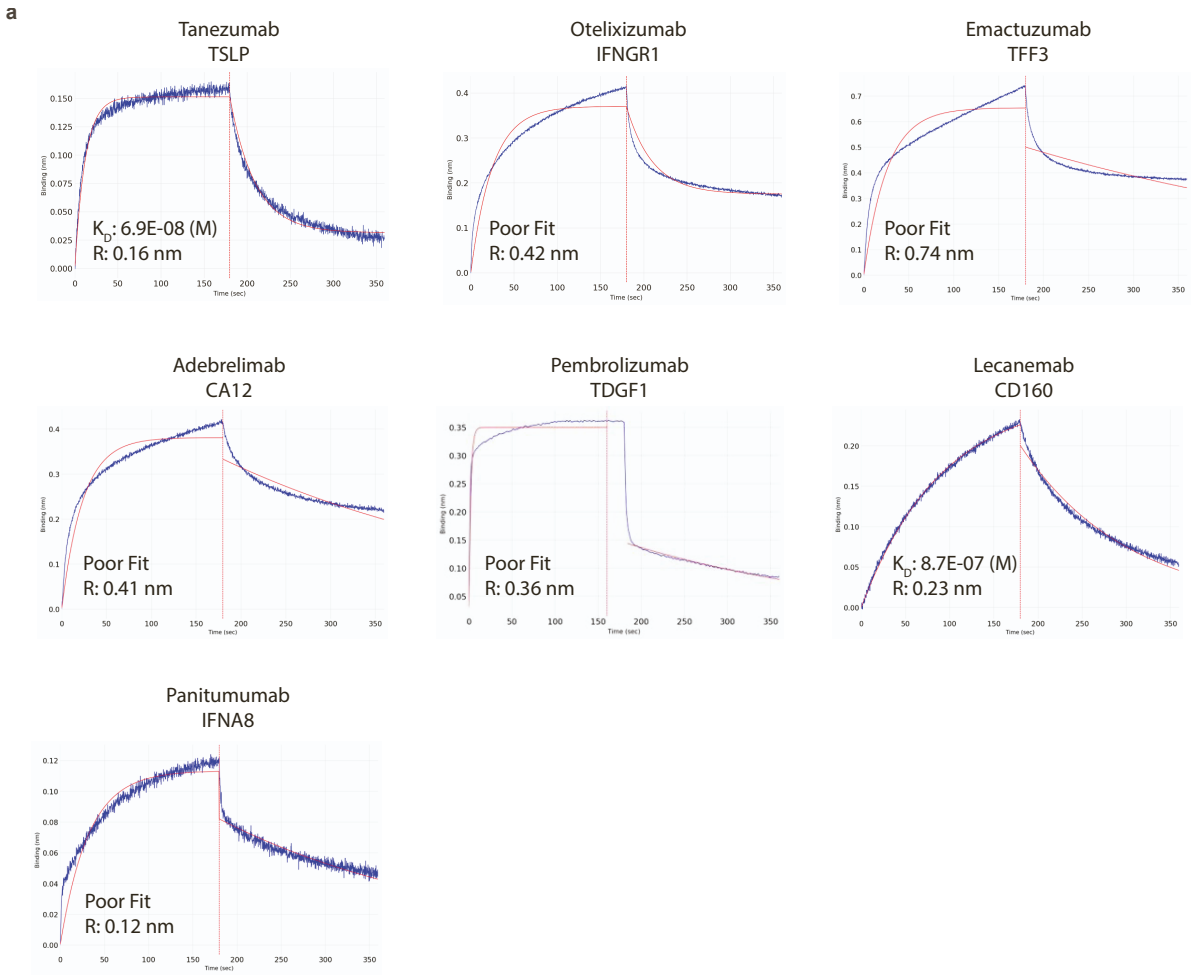

Figure S2. **Characterization of IgG binding interactions identified by REAP. Related to Figure 2, Figure 3 and Table 1.** Biolayer interferometry (BLI) assay showing binding of IgGs to proteins identified from REAP screen in an avid assay format. Each sensorgram is titled with the antibody and associated interacting protein. Poor Fit indicates profiles which do not fit to a 1:1 binding model. R = response.

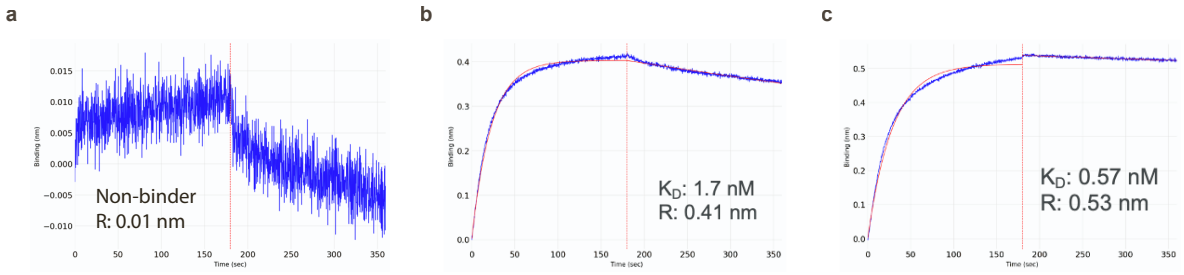

Figure S3. Binding of tanezumab, TSLPR, and tezepelumab to TSLP as measured by BLI assay. Related to Figure 3. (a) Tanezumab does not display monovalent binding to TSLP (tanezumab IgG loaded on sensor and TSLP monomer in solution). (b) TSLP-Fc dimer binds to sensor-immobilized TSLPR-Fc dimer. (c) Sensor-immobilized tezepelumab binds to TSLP-Fc dimer in solution. R = response.

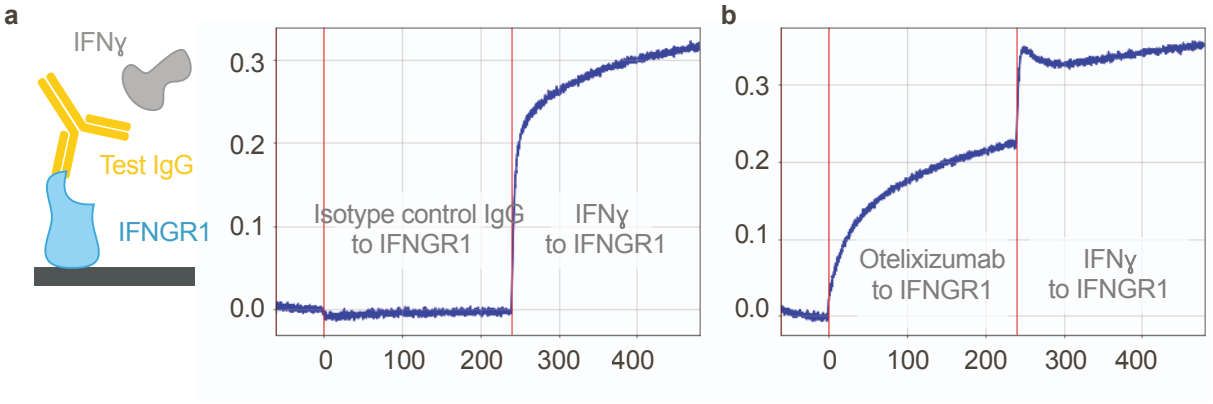

Figure S4. Biophysical characterization of the off-target reactivity of otelixizumab and IFNGR1. Related to Figure 3. (a) An isotype negative control IgG does not bind to immobilized IFNGR1 or inhibit binding of IFNγ to IFNGR1. (b) Otelixizumab binds to immobilized IFNGR1 but does not inhibit binding of IFNγ to IFNGR.